2024SPSBIC0034

Analytical Investigation of Thermal Stratification in the Flow of Fluid in a Cylindrical Pipe

Yahaya, H. M.[1*], Yusuf, S. I.[2], Jimoh, O. R.[3] and Abubakar, A. D.[4]
[1, 2, 3] Department of Mathematics, Federal University of Technology Minna, Niger State.
[4] Department of Mathematics, Federal University Gashua, Yobe State
[1*]yahayahabiba084@gmail.com,

Abstract

Thermal stratification is a phenomenon where a hot layer of fluid flows over a cold layer of fluid due to density difference. This research work investigates the effect of thermal stratification on fluid flow in a horizontal circular pipe. The transient behaviours of fluid flow, velocity and temperature distribution in the pipe were analysed using Olayiwola's generalized polynomial approximation method (OGPAM). It was found that Grashof's number increases the velocity of the fluid. It was also observed that Peclet number, Biot number and Eckert number decrease the temperature of the fluid and at later time increase as the values of these parameters increase. The results also show that the thermal stratification parameter reduces the temperature profile.

Keywords: Thermal, OGPAM, cylindrical pipe, stratification, Biot number.

1. Introduction

Thermal stratification is a phenomenon where a hot layer of fluid flows over a cold layer of fluid due to their differences in density. In piping systems where hot and cold fluids flow in, two fluid layers can be formed due to the difference in fluid density or temperature. Such phenomenon is called thermal stratification. Where this is the case, the cold (denser) fluid occupies the lower position of the pipe, while the hot fluid occupies the upper space. This condition may lead to considerable circumferential temperature gradient in the pipe wall, which can eventually result in excessive differential expansion at the top and bottom of the pipe threatening the integrity of the piping system. (Jo, 2001). The thermally induced damage inflow regimes can occur in high-temperature environments and thermal cycling. Thermal striping, and thermal stratification are the most common causes of thermally induced damage. It usually happens in constrained flow regimes where the fluid is moving at a low velocity and has a considerable temperature variation. When two types of steam with different temperatures come into contact, thermal stratification occurs. Due to the temperature differential, the heavier water sinks being colder, while the lighter and warmer water floats over the colder water. One of the most important aspects of thermal stratification for anglers is that the lowest layer of water, which is deprived of surface contact, loses dissolved oxygen and becomes less capable of supporting aquatic life (Rehman & Shatanawi 2022). Many factors such as solar radiation, air temperature, wind speed, water density, specific heat and cyano bacterial bloom and others impact on thermal stratification. With the increase of solar radiation intensity, the vertical profile of water temperature rises at first and then drops (Jin *et al.* 2018).

Rehman *et al.* (2020) carried out the analysis of thermally stratified flow of Sutterby nanofluid with zero mass flux condition. It was found that increase in fluid parameter declines the velocity field whereas temperature field rises for higher thermal conductivity parameter. The magneto-hydrodynamic of thermal and solutal stratified stagnation flow of tangent hyperbolic fluid induced by stretching cylinder with dual convection was investigated by Choudhary *et al.* (2023). The flow-narrating differential equations, which are constrained by a thermal and solutal stratified porous medium, are transmuted into a system of nonlinear differential equations and solved numerically. Their observation shows that in the appearance of Joule heating, the fluid temperature is a lowering function of thermal stratification. Also, the findings are compared with the existing literature and found to be consistent with earlier research of (Rehman *et al.* 2018). Duraihem *et al.* (2023) investigated thermal stratification effect on gravity driven transport of hybrid carbon nanotubes (CNTs) down a stretched surface through

porous medium. The findings showed that the presence of hybrid carbon nanotubes and medium porosity contributes significantly to upsurging surface shear stress magnitude whereas, external magnetic field and velocity slip effects in an altered manner. A comparative remark on heat transfer in thermally stratified MHD Jeffrey fluid flow with thermal radiations subject to cylindrical/plane surfaces was investigated by Rehman *et al.* (2022). Their findings showed that thermo-physical flow field aspects are enriched for magnetized stratified convective flow towards the cylindrical surface as compared to a plane surface. Gao *et al*. (2021) performed both experimental and numerical investigations on thermal stratification characteristics affected by the baffle plate in thermal storage tank. Response surface method was used to optimize the structure parameters. The temperature field and flow field inside the storage tank were calculated by numerical simulation, and the effects of different structural parameters on the mixing number, stratification number, and the Richardson number were analysed. The results showed that the three evaluation indices correspond to different optimal parameter combinations. While, the interaction factors that have a crucial influence on the three evaluation indices are baffle aperture and inlet velocity, baffle position and inlet velocity, baffle position and baffle aperture. Chen *et al.* (2018) used numerical simulation and experimental methods to study the heat transfer and temperature stratification of a rectangular water tank in a solar hot water system under different flow conditions. The size of the water tank was 450 × 400 × 500 mm and 15 layers of coils were arranged in the canter of the water tank. The experimental results verified the correctness of the simulation results. In addition, the flow field analysis showed that the heat transfer mechanism, thermal stratification, runoff time, buoyancy, mixing process and tank geometry are closely related. The results showed that the shell-side Nusselt number increases with the increase in the Reynolds number and a correlation formula for predicting the shell-side Nusselt number was proposed. Yusuf *et al.* (2019) carried out a mathematical analysis of discontinuities in the flow field of gas in a cylindrical pipe using diffusion MRI. Their results show that for free fluid flow, the magnetization is between 0.004 and 0.005. For partial blockage, the magnetization reduces (signal loss) in value to 0.00001 and for total blockage it is zero (0). Their analysis can also be useful in process industries where different network of pipes are used or machines use cylindrical pipes or tubes in transporting materials especially when there is a partial or total blockage at any point in the network.

Assari *et al*. (2018) carried out experiments on the damage of the thermal stratification of the storage tank and its influence on the performance of the solar collector. The result shows that the temperature at the bottom of the tank is inversely proportional to the efficiency of the collector and the simulation results are in good agreement with the experimental results. More so, insight into significance of thermal stratification and radiation on dynamics of micropolar water based TiO_2 nanoparticle via finite element simulation was investigated. Findings from this study indicated a decline on temperature field due to increasing values of the thermal stratification parameter (Ali *et al.* 2022). Our aim is to investigate the effect of thermal stratication in the flow of fluid in a cylindrical pipe which is an extension of Gao *et al.* (2021).

2. Model Formulation

An unsteady, incompressible viscous flow past a finite cylindrical pipe of radius r with constant temperature in the presence of thermal stratification is being considered. The flow is one-dimensional in a horizontal pipe. The velocities along θ and Z are assumed to be constant.
Considering the above assumptions, the governing equations are as follows.

2.1 Momentum equation

$$\rho\left(\frac{\partial V_r}{\partial t'}+V_r\frac{\partial V_r}{\partial r'}\right)=-\frac{\partial p}{\partial r'}+\frac{\mu}{r'}\frac{\partial}{\partial r'}\left(r'\frac{\partial V_r}{\partial r'}\right)+\rho g\beta\left(T-T_\infty\right),$$

$$V_r\left(r',\ 0\right)=U_o,\quad \left.\frac{\partial V_r}{\partial r'}\right|_{r'=0}=U_o,\qquad \left.\frac{\partial V_r}{\partial r'}\right|_{r'=1}=0.$$

(1)

2.2 Energy equation

$$\rho C_p\left(\frac{\partial T}{\partial t'}+V_r\frac{\partial T}{\partial r'}\right)=\frac{k}{r'}\frac{\partial}{\partial r'}\left(r'\frac{\partial T}{\partial r'}\right)+\mu\left(\frac{\partial V_r}{\partial r'}\right)^2-\gamma V_r,$$

$$T\left(r',\ 0\right)=T_\infty,\quad \left.\frac{\partial T}{\partial r'}\right|_{r'=0}=0,\qquad -k_s\left.\frac{\partial V_r}{\partial r'}\right|_{r'=1}=h_f\left(T\left(R,\ t'\right)-T_\infty\right).$$

(2)

where,

V_r and T are the velocity and temperature of the fluid respectively, t' is the time, r' stands for the radial coordinate, ρ is the density of the fluid, C_p is the specific capacity, g is the acceleration due to gravity, γ is the thermal stratification parameter, μ is kinematic viscousity, T_∞ is the temperature at the surface of the pipe, β Volumetric coefficient of thermal expansion, k is the thermal diffusivity, h_f is the convective heat transfer coefficient at the fluid phase, k_s is the thermal conductivity at the solid phase and U_0 is the velocity at the initial point.

2.3 Method of Solution

2.3.1 Dimensional analysis

Dimensionless variables are been introduced as:

$$t=\frac{U_o t'}{R},\quad r=\frac{r'}{R},\quad u=\frac{V_r}{U_o},\quad \theta=\frac{T-T_o}{T_\infty-T_o}.$$

(3)

Substituting (3), into (1) – (2), we obtained in dimensionless form as:

$$\frac{\partial u}{\partial t}+u\frac{\partial u}{\partial r}=-\alpha_0\frac{\partial p}{\partial r}+\frac{1}{\mathrm{Re}}\frac{1}{r}\frac{\partial}{\partial r}\left(r\frac{\partial u}{\partial r}\right)+Gr_\theta\theta,$$

$$u\left(r,\ 0\right)=1,\quad \left.\frac{\partial u}{\partial r}\right|_{r=0}=1,\qquad \left.\frac{\partial u}{\partial r}\right|_{r=1}=0.$$

(4)

$$\frac{\partial \theta}{\partial t}+u\frac{\partial \theta}{\partial r}=\Pr\frac{1}{r}\frac{\partial}{\partial r}\left(r\frac{\partial \theta}{\partial r}\right)+Ec\left(\frac{\partial u}{\partial r}\right)^2-\alpha_1 u,$$

$$\theta(r,\ 0)=1,\quad \left.\frac{\partial \theta}{\partial r}\right|_{r=0}=0,\qquad -\left.\frac{\partial \theta}{\partial r}\right|_{r=1}-Bi\,\theta(1,\ t)=-Bi.$$

(5)

where,

$\alpha_0=\dfrac{1}{U_0^2\rho}$, $\mathrm{Re}=\dfrac{\mu}{RU_0\rho}=$ Reynolds number, $\Pr=\dfrac{k}{\rho C_p RU_0}=$ Prandtl number, $Bi=\dfrac{Rh_f}{k_s}=$ Biot number, $Ec=\dfrac{\mu U_0}{R\rho C_p(T_\infty-T_0)}=$ Eckert number, $Gr_\theta=\dfrac{Rg\beta(T_\infty-T_0)}{U_0^2}=$ Thermal Grashof's number, $\alpha_1=\dfrac{\gamma R}{\rho C_p(T_\alpha-T_0)}=$ Thermal stratification.

2.3.2 Analytical solution via OGPAM

Let

$$\frac{\partial p}{\partial r}=\lambda e^{-\alpha t}\quad \text{and}\quad 0<Gr_\theta<1$$

(6)

However, in many practical applications, Gr_θ cannot be zero $(Gr_\theta\neq 0)$, but in many situations it can take small values Choudhary, *et al.* (2023) and Rashid, *et al.* (2020). Small value of $Gr_\theta<1$ facilitate finding solutions of equations (4) and (5) by using perturbation method in the form:

$$\left.\begin{aligned}u&=u_0+Gr_\theta u_1+\ldots\\ \theta&=\theta_0+Gr_\theta\theta_1+\ldots\end{aligned}\right\}$$

(7)

equations (4) and (5) were solve analytically using OGPAM (Olayiwola, 2022), and obtained as follows:

$$\begin{aligned}u(r,t)=&\left(r-\frac{r^2}{2}-\frac{1}{2}+A_0\exp\left(\frac{1}{3}\right)t+B_0\exp(-\alpha)t-C_0\right)+\\ &Gr_\theta\left(A_6+B_6t+C_6t^2+D_6t^3-E_6t^4-F_5t^5+F_6e^{-t}+G_6e^{-C_3t}+H_6te^{-C_3t}+J_6t^2e^{-C_3t}\right)+\ldots\end{aligned}\tag{8}$$

$$\theta(r,t)=\begin{pmatrix}\left(\left(1+\frac{Bi}{2}\right)\begin{pmatrix}A_4e^{-\left(C_3t+D_3t^2\right)}+B_4e^{-D_3t^2}+C_4te^{-D_3t^2}+D_4t^2e^{-D_3t^2}\\+E_4t^3e^{-D_3t^2}\end{pmatrix}-\frac{Bi}{2}\right)-\\ \frac{Bi}{2}\left(\left(A_4e^{-\left(C_3t+D_3t^2\right)}+B_4e^{-D_3t^2}+C_4te^{-D_3t^2}+D_4t^2e^{-D_3t^2}+E_4t^3e^{-D_3t^2}\right)-1\right)r^2.\end{pmatrix}+$$

$$Gr_\theta\begin{pmatrix}\left(1+\frac{Bi}{2}\right)\begin{pmatrix}\left(A_8+B_8t+C_8t^2+D_8t^3+E_8t^4+F_8t^5+G_8t^6+H_8t^7\right)e^{-D_3t^2}\\+J_8e^{-\left(C_3t+D_3t^2\right)}\end{pmatrix}\\ -\frac{Bi}{2}\begin{pmatrix}\left(A_8+B_8t+C_8t^2+D_8t^3+E_8t^4+F_8t^5+G_8t^6+H_8t^7\right)e^{-D_3t^2}\\+J_8e^{-\left(C_3t+D_3t^2\right)}\end{pmatrix}r^2.\end{pmatrix}+\ldots \tag{9}$$

where,

$$A_0=\left(\frac{-3\alpha_0\lambda}{3\alpha+1}+\frac{3}{20}+1\right),\quad B_0=\frac{3\alpha_0\lambda}{3\alpha+1},\quad C_0=\frac{3}{20}$$

$$A_1=\frac{4}{4+Bi}\left(\frac{2BiA_0}{3}\right),\quad B_1=\frac{4}{4+Bi}\left(\frac{2BiB_0}{3}\right),\quad C_1=\frac{4}{4+Bi}\left(Bi\left(\frac{60+Pe}{30Pe}\right)+\frac{2BiC}{3}\right),$$

$$A_2=\frac{4}{4+Bi}\left(\frac{2Bi}{3}-\alpha_1\right)A_0,\quad B_2=\frac{4}{4+Bi}\left(\frac{2Bi}{3}-\alpha_1\right)B_0,$$

$$C_2=\frac{4}{4+Bi}\left(Bi\left(\frac{60-Pe}{30Pe}\right)+\frac{Ec}{6}+\frac{11\alpha_1}{12}-\left(\frac{2Bi}{3}-\alpha_1\right)C_0\right),$$

$$A_5=\left(\left(\frac{2Bi+6}{3}\right)B_4-\frac{2Bi}{3}\right),\quad B_5=\left(\frac{2Bi+6}{3}\right)C_4,\quad C_5=\left(\frac{2Bi+6}{3}\right)\left(D_3-B_4D_3\right),$$

$$D_5=\left(\frac{2Bi+6}{3}\right)\left(E_4-C_4D_3\right),\quad E_5=\left(\frac{2Bi+6}{3}\right)D_3D_4,\quad F_5=\left(\frac{2Bi+6}{3}\right)D_3E_4,$$

$$G_5=\left(\frac{2Bi+6}{3}\right)A_4,\quad H_5=\left(\frac{2Bi+6}{3}\right)A_4D_3,\quad A_6=\begin{pmatrix}A_5-B_5+2C_5-6D_5-24E_5\\+120F_5\end{pmatrix},$$

$$B_6=\left(B_5-2C_5+6D_5+24E_5-120F_5\right),\quad C_6=\left(C_5-3D_5-12E_5+60F_5\right),$$

$$D_6=\left(D_5+4E_5-20F_5\right),\quad E_6=\left(E_5-5F_5\right),$$

$$F_6=\left(B_5-A_5-2C_5+6D_5+24E_5-120F_5+\frac{G_5}{(C_3-1)}-\frac{2H_5}{C_3^3-3C_3^2+3C_3-1}\right),$$

$$G_6=\left(\frac{2H_5}{C_3^3-3C_3^2+3C_3-1}-\frac{G_5}{(C_3-1)}\right),\ H_6=\left(\frac{(2C_3-2)H_5}{C_3^3-3C_3^2+3C_3-1}\right),\ J_6=\left(\frac{(C_3^2-2C_3+1)H_5}{C_3^3-3C_3^2+3C_3-1}\right).$$

$$A_7=\frac{4}{4+Bi}\left(\frac{2Bi}{3}(A_4A_6+A_4F_6+A_4G_6+B_4A_6+B_4F_6+B_4G_6)-\left(\frac{\alpha_1}{2}+\frac{2Bi}{3}\right)(A_6+F_6+G_6)\right),$$

$$B_7=\frac{4}{4+Bi}\left(\begin{array}{l}\frac{2Bi}{3}\left(\begin{array}{l}-A_4A_6C_3+A_4B_6-A_4F_6(C_3+1)-2A_7G_7C_3+A_4H_6+B_4B_6\\-B_4F_6-B_4G_6C_3+B_4H_6+C_4A_6+C_4F_6+C_4G_6\end{array}\right)-\\\left(\frac{\alpha_1}{2}+\frac{2Bi}{3}\right)(B_6-F_6-G_6C_3+H_6)\end{array}\right),$$

$$C_7=\frac{4}{4+Bi}\left(\begin{array}{l}\frac{2Bi}{3}\left(\begin{array}{l}-A_4A_6D_3-A_4B_6C_3+A_4C_6-A_4F_6D_3-A_4G_6D_3-2A_4H_6C_3\\+A_4J_6-B_4A_6D_3+B_4C_6-B_4F_6D_3-B_4G_6D_3-B_4H_6C_3+B_4J_6\\+B_6C_4-C_4F_6-C_4G_6C_3+C_4H_6+D_4A_6+D_4F_6+D_4G_6\end{array}\right)-\\\left(\frac{\alpha_1}{2}+\frac{2Bi}{3}\right)(C_6-H_6C_3+J_6)\end{array}\right),$$

$$D_7=\frac{4}{4+Bi}\left(\begin{array}{l}\frac{2Bi}{3}\left(\begin{array}{l}-A_4B_6D_3-A_4C_6C_3+A_4D_6-A_4H_6D_3-2A_4J_6C_3-B_4B_6D_3\\+A_4D_6-B_4H_6D_3+C_4C_6-B_4J_6D_3-C_4A_6D_3-C_4F_6C_3-\\C_4G_6D_3-C_4H_6C_4+C_4J_6+D_4E_6-D_4H_6-D_4G_6C_3+D_4H_6+\\E_4A_6+E_4F_6+E_4G_6\end{array}\right)-\\\left(\frac{\alpha_1}{2}+\frac{2Bi}{3}\right)(D_6-J_6C_3)\end{array}\right),$$

$$E_7=\frac{4}{4+Bi}\left(\begin{array}{l}\frac{2Bi}{3}\left(\begin{array}{l}-A_4C_6D_3-A_4D_6C_3-A_4E_6-A_4J_6D_3-B_4C_6D_3-B_4E_6-B_4J_6D_3\\-C_4B_6D_3-C_4C_6D_3+C_4D_6-C_4H_6D_3-C_4J_6C_3-D_4A_6D_3+D_4C_6\\-D_4F_6D_3-D_4G_6D_3-D_4H_6C_3+D_4J_6+E_4B_6-E_4F_6-E_4G_6C_3+\\E_4H_6\end{array}\right)\\+\left(\frac{\alpha_1}{2}+\frac{2Bi}{3}\right)E_6\end{array}\right),$$

$$F_7 = \frac{4}{4+Bi}\left(\begin{array}{l}\frac{2Bi}{3}\left(\begin{array}{l}-A_4D_6D_3 + A_4E_6C_3 - A_4F_5 - B_4D_6D_3 - B_4F_5 - C_4E_6 - C_4J_6D_3\\ -D_4B_6D_3 - D_4B_6D_3 + D_4D_6 - D_4H_6D_3 - D_4J_6C_3 - E_4A_6D_3 + E_4C_6\\ -E_4F_6D_3 - E_4G_6D_3 - E_4H_6C_3 + E_4J_6\end{array}\right)\\ +\left(\frac{\alpha_1}{2}+\frac{2Bi}{3}\right)F_5\end{array}\right),$$

$$A_8 = \left(\begin{array}{l}\frac{A_5}{C_3} - \frac{B_7}{C_3^2} + \frac{2(A_7D_3+C_7)}{C_3^3} - \frac{6(B_7D_3+D_7)}{C_3^4} + \frac{24(C_7D_3+E_7)}{C_3^5} - \frac{120(D_7D_3+F_7)}{C_3^5} +\\ \frac{720E_7}{C_3^7} - \frac{5040F_7}{C_3^8}\end{array}\right),$$

$$B_8 = \left(\begin{array}{l}\frac{B_7C_3}{C_3^2} - \frac{2C_3(A_7D_3+C_7)}{C_3^3} + \frac{6C_3(B_7D_3+D_7)}{C_3^4} - \frac{24C_3(C_7D_3+E_7)}{C_3^5} +\\ \frac{120C_3(D_7D_3+F_7)}{C_3^5} - \frac{120(D_7D_3+F_7)}{C_3^6} - \frac{720C_3E_7}{C_3^7} + \frac{504C_3E_7}{C_3^8}\end{array}\right),$$

$$C_8 = \left(\begin{array}{l}\frac{C_3^2(A_7D_3+C_7)}{C_3^3} - \frac{3C_3^2(B_7D_3+D_7)}{C_3^4} + \frac{12C_3^2(C_7D_3+E_7)}{C_3^5} - \frac{60C_{33}^2(D_7D_3+F_7)}{C_3^6}\\ +\frac{360C_3^2E_7}{C_3^7} - \frac{2550C_3^2F_7}{C_3^8}\end{array}\right),$$

$$D_8 = \left(\frac{C_3^3(B_7D_3+D_7)}{C_3^4} - \frac{4C_3^3(C_7D_3+E_7)}{C_3^5} + \frac{20C_3^3(D_7D_3+F_7)}{C_3^6} - \frac{120C_3^3E_7}{C_3^7} + \frac{840C_3^3F_7}{C_3^8}\right),$$

$$E_8 = \left(\frac{C_3^4(C_7D_3+E_7)}{C_3^5} - \frac{5C_3^4(D_7D_3+F_7)}{C_3^6} + \frac{30C_3^4E_7}{C_3^7} - \frac{210C_3^4F_7}{C_3^8}\right), \quad J_8 = -A_8$$

$$F_8 = \left(\frac{C_3^5(D_7D_3+F_7)}{C_3^6} - \frac{6C_3^5E_7}{C_3^7} + \frac{42C_3^5F_7}{C_3^8}\right), \quad G_8 = \frac{C_3^{56}E_7}{C_3^7} - \frac{7C_3^7F_7}{C_3^8}, \quad H_8 = \frac{C_3^7F_7}{C_3^8},$$

3. Results and Discussion

In this work, the governing equations (4) and (5) were solved using Olayiwola's Generalized Polynomial Approximation Method. The solutions are computed for the values of $Ec = 0.5,\ Gr_\theta = 0.01,\ Pe = 0.3,\ \mathrm{Re} = 0.2,\ \alpha_1 = 0.2, Bi = 0.1$.The impact of various physical parameters on the flow characteristics (velocity and temperature,) are graphically displayed in figures 1 – 9.

Figures 1 and 2 show the variation of velocity with thermal Grashof's number Gr_θ at $\lambda = 1$, (positive pressure gradient). Gr_θ is the ratio of thermal buoyancy to viscous forces within the fluid. It was observed from these figures that the velocity increases both along distance and time. This is due to an increase in buoyancy forces as well as a decrease in viscous forces. The internal resistance of the fluid tend to decrease upon a decrease in the viscosity, which causes an increase in the fluid velocity thereafter. A similar effect of this parameter can be found in (Venkateswarlu *et al.* 2019) who studied the Influence of heat generation and viscous dissipation on hydromagnetic fully developed natural convection flow in a vertical micro-channel and (Kumar *et al.* 2021). Figures 3 and 4 represent temperature profiles at $\lambda = 1$. It was observed that increase in the value of Echert number Ec, increases the temperature. But reduces along distance and increases with time. This is due to the heat generated by the internal friction within the fluid which increases the rate of heat transfer. Similar findings have been reported by (Kishore *et al.* 2010) who studied the effects of heat transfer and viscous dissipation on Magnetohydrodynamic (MHD) free convection flow past an exponentially accelerated vertical plate with variable temperature.

Figures 5 and 6 shows the variation of temperature with thermal stratification α_1 at $\lambda = 1$. It was observed that increase in the value of α_1, decreases the temperature along distance and increases with time. This is because the fluid with dense stratification in the pipe is lower than the ambient temperature**.** This type of behaviour has also been observed by Paul and Dekar (2017), Madhu *et al.* (2015) and (Choudhary, *et al.* 2023). Figures 7 and 8 depict the effects of Peclet number Pe on temperature profile at $\lambda = 1$, (positive pressure gradient). Pe measures the relative importance of convective flux to diffusive flux. A high temperature was observed at the initial point but decreases along distance and increases with time. The maximum fluid temperature is also obtained as the value of Pe increases. A similar behavior of this parameter has been reported by Muritala *et al.* (2021) who studied heat transfer in microchannels. Figure 9 show the variation of temperature profile with Biot number Bi at $\lambda = 1$ .Biot number is the ratio of the internal thermal resistance of a solid to the boundary layer thermal resistance. It was observed from this figure that temperature decreases along distance and increases with time. However, increasing the parameter values, increases the temperature.

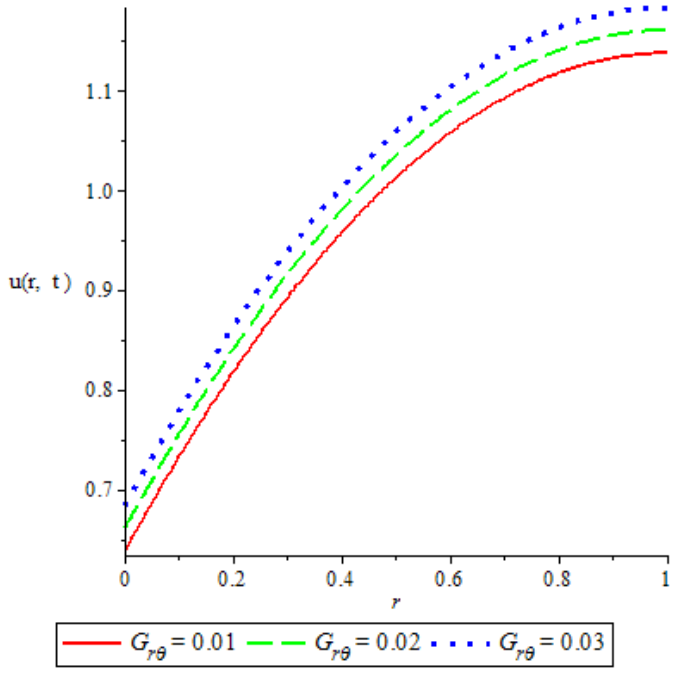

Figure 1: Variation of velocity with thermal Grashof's number Gr_θ against distance

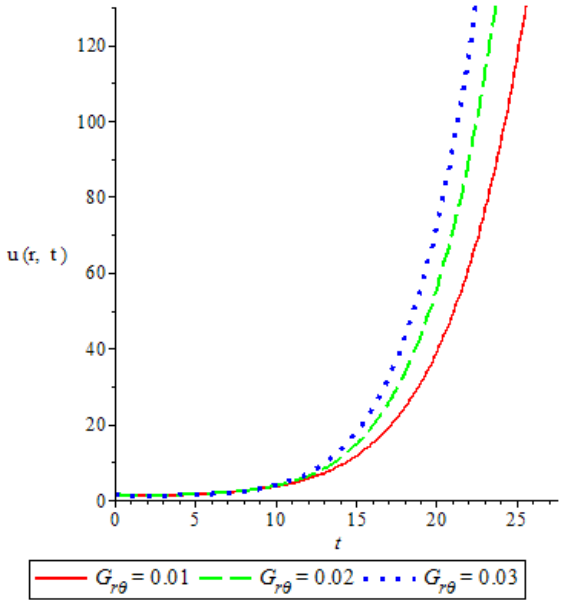

Figure 2: Variation of velocity with thermal Grashof's number Gr_θ against time

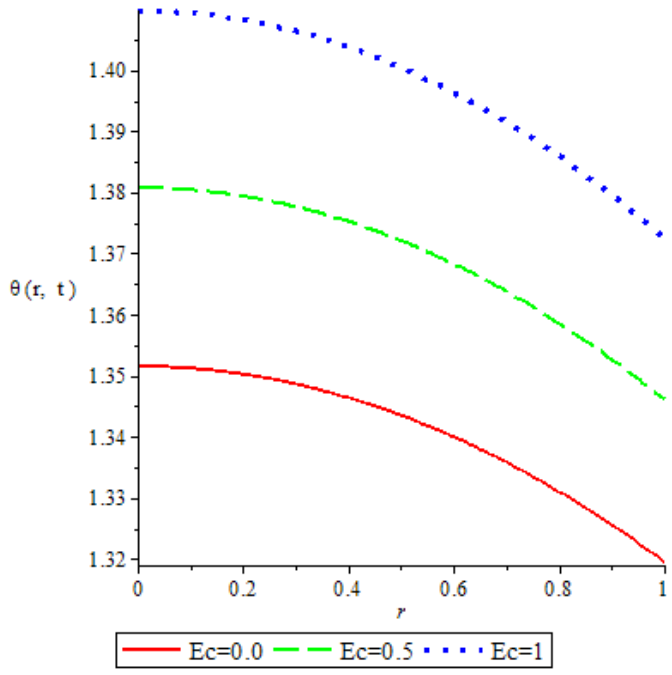

Figure 3: Effect of Eckert number on temperature against distance

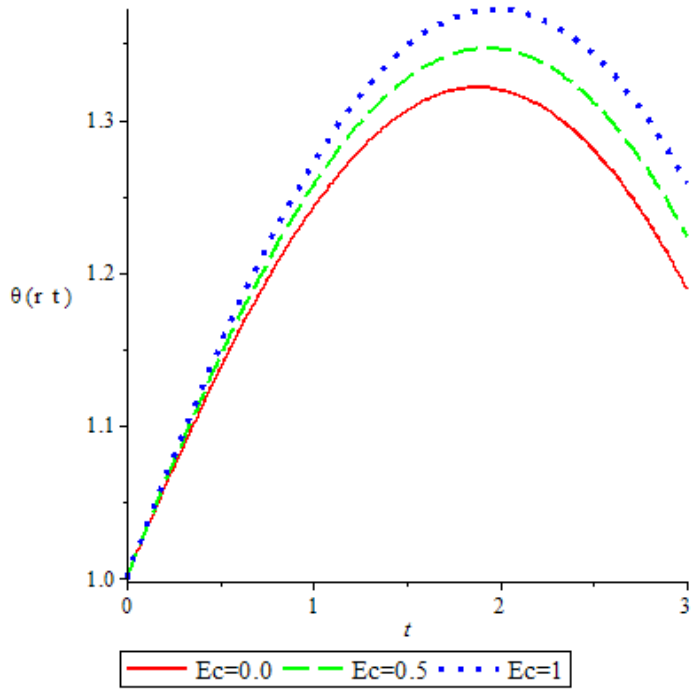

Figure 4: Effect of Eckert number on temperature against time

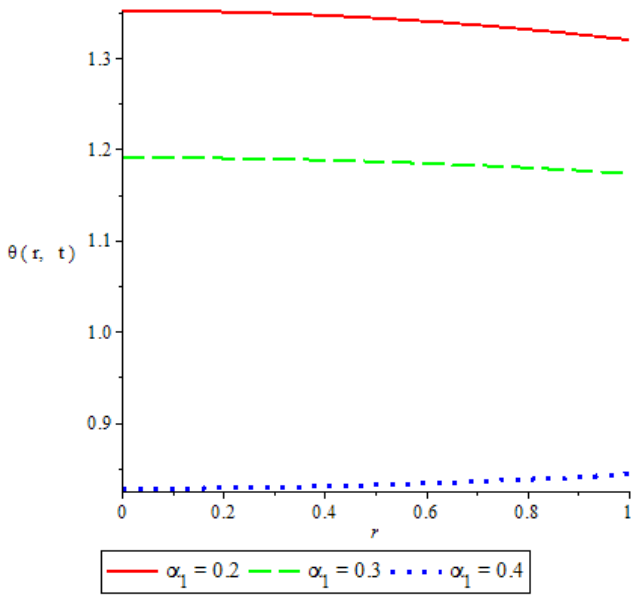

Figure 5: Effect of thermal stratification on temperature against distance

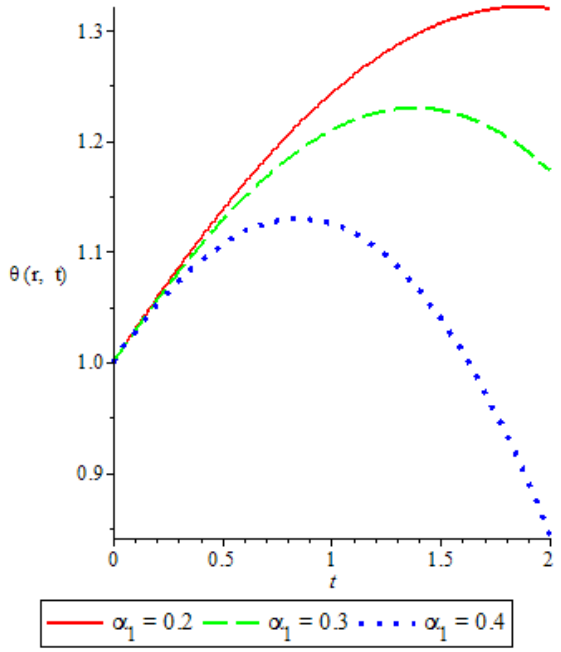

Figure 6: Effect of thermal stratification on temperature against time

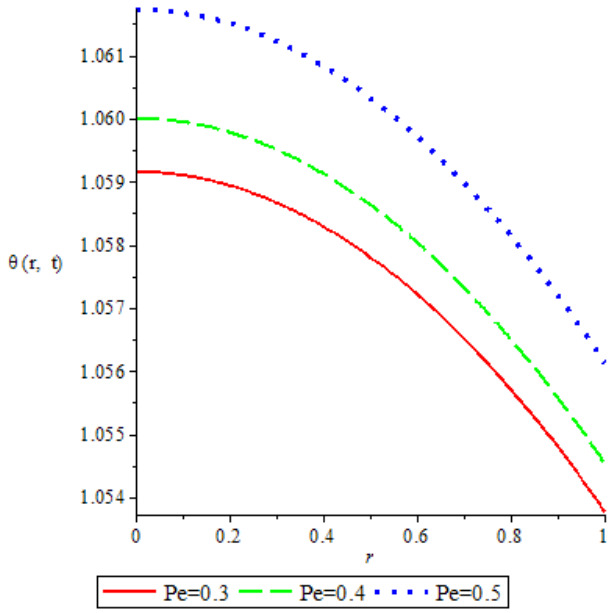

Figure 7: Variation of temperature with Pecletl number Pe against distance

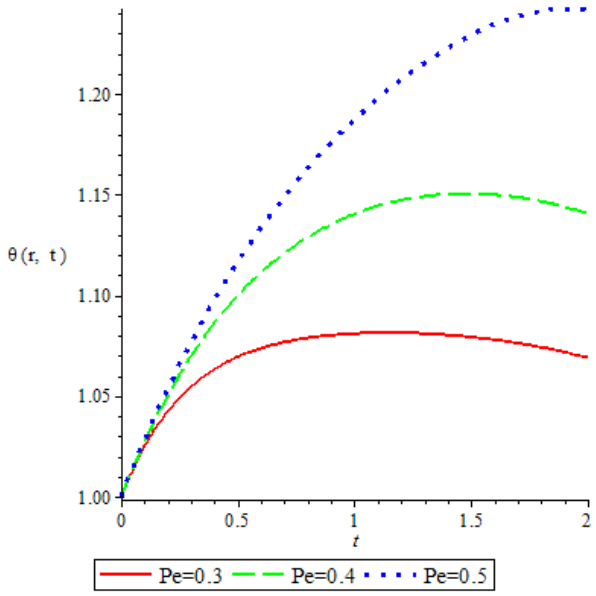

Figure 8: Variation of temperature with Peclet number Pe against time

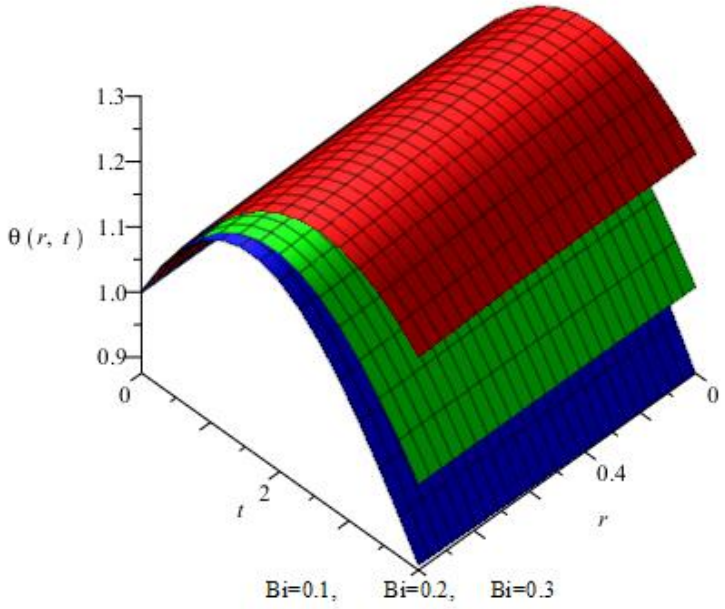

Figure 9: Effect of Biot number on temperature against distance and time

4. Conclusion

In summary, fluid flow in a cylindrical pipe was investigated analytically which determines the effect of thermal stratification. The study observed from the existing literatures that environment is thermally stratified in many mixed flows of practical importance in nature as well as in many engineering devices.

The discharge of hot fluid into enclosed regions often results in a stable thermal stratification with lighter fluid overlying denser fluid. The study is applicable in industries when conveying fluid from one point to another as well as in an environmental media, such as rivers and lakes. Also, in the migration of underground water and water purification processes. OGPAM is very effective in analyzing parabolic equations with constant or variable coefficients in the cases of slab, cylindrical or spherical geometries under consideration, unlike other methods that are only applicable to equations with constant coefficient and a particular geometry. The findings and outcomes of this research work are recommended to geophysicists and other scientists in related disciplines as it will assist greatly in the study of interaction of the geomagnetic field with the fluid in the geothermal regions.

REFERENCE

Ali, L., Ali, B., Mousa, A. A., Hammouch, Z., Hussain, S., Siddique, I. & Huang, Y. (2022). Insight into significance of thermal stratification and radiation on dynamics of micropolar water based TiO_2 nanoparticle via finite element simulation. *Journal of material research and technology,* 19:4209–4219.

Assari, M.R., Basirat Tabrizi, H. & Movahedi, M. J. (2018). Experimental study on destruction of thermal stratification tank in solar collector performance. J*ournal of Energy Storage*, 15, 124–132, https://doi.org/10.1016/j.est.2017.11.004.

Chen, J., Xu, H.T. & Wang, Z.Y. (2018). Thermal performance study of a water tank for a solar system with a fresnel lens. *Journal of Solar Energy Engineering*, 140 (5), 051005.

Choudhary, S., Choudhary, P., Alessa, N. & Loganathan, K. (2023). MHD thermal and solutal stratified stagnation flow of tangent hyperbolic fluid induced by stretching cylinder with dual convection. *Mathematics*, 11, 2182. https://doi.org/10.3390/math11092182.

Duraihem, F. Z., Maraj, E.N., Akbar, N. S. & Mehmood, R. (2023). Thermal stratification effect on gravity driven transport of hybrid CNTs down a stretched surface through porous medium. *Heliyon*, 9, e15699.

Gao, L., Lu, H., Sun, B., Che, D. & Dong, L. (2021). Numerical and experimental investigation on thermal stratification characteristics affected by the baffle plate in thermal storage tank. *Journal of Energy Storage*, 34, 102117.

Jin, J., Scott, Wells, S. A., Liu, D. & Yang, G. (2018). Thermal stratification and its relationship with water quality in the typical tributary bay of the Three Gorges Reservoir, *Water Supply,* 19(3), 918-925.http://doi.org/10.2166/ws.2018.142.

Jo, J. C., Kim, Y. & Choi, S. K. (2001). Numerical Analysis of Thermal Stratification in a Circular Pipe. *Journal of Pressure Vessel Technology*, 123/517.

Kishore P. M, Rajash V. & Vijayakumar V. S. (2010). Effects of heat transfer and viscous dissipation on MHD free convection flow past an exponentially accelerated vertical plate with variable temperature. *Journal of Naval Architecture and Marine Engineering. 7, 101-110.*

Kumar, M. A., Reddy, Y. D., Goud, B. S., & Rao, V. S. (2021). Effects of soret, dufour, hall current and rotation on MHD natural convective heat and mass transfer flow past an accelerated vertical plate through a porous medium. *International Journal of Thermofluids*, 9, 100061.

Madhu, J. V., Rajasekhar, M. N. & Reddy, B. S. (2015). Effects of viscous dissipation and thermal stratification on chemical reacting fluid flow over a vertical stretching surface with heat source. *Advances in Applied Science Research*, 6(1): 59-65.

Muritala, F, Olayiwola, R. O, Oyedeji, A. A., & Akande, S. O. (2021). Mathematical modelling of heat transfer in microchannels. *Journal of Science, Technology, Mathematics and Education (JOSTMED),* 17(3), 81 – 87.